

Alma Mater Studiorum Università di Bologna  
Archivio istituzionale della ricerca

Expanding the spectrum of polydopamine antioxidant activity by nitroxide conjugation

This is the final peer-reviewed author's accepted manuscript (postprint) of the following publication:

*Published Version:*

Mollica F., Lucernati R., Amorati R. (2021). Expanding the spectrum of polydopamine antioxidant activity by nitroxide conjugation. JOURNAL OF MATERIALS CHEMISTRY. B, 9(48), 9980-9988 [10.1039/d1tb02154k].

*Availability:*

This version is available at: <https://hdl.handle.net/11585/847280> since: 2023-02-24

*Published:*

DOI: <http://doi.org/10.1039/d1tb02154k>

*Terms of use:*

Some rights reserved. The terms and conditions for the reuse of this version of the manuscript are specified in the publishing policy. For all terms of use and more information see the publisher's website.

This item was downloaded from IRIS Università di Bologna (<https://cris.unibo.it/>).  
When citing, please refer to the published version.

(Article begins on next page)

This is the final peer-reviewed accepted manuscript of:

Fabio Mollica, Rosa Lucernati and Riccardo Amorati

Expanding the spectrum of polydopamine antioxidant activity by nitroxide conjugation

J. Mater. Chem. B, 2021,9, 9980

The final published version is available online at: DOI: 10.1039/d1tb02154k

#### Rights / License:

The terms and conditions for the reuse of this version of the manuscript are specified in the publishing policy. For all terms of use and more information see the publisher's website.

*This item was downloaded from IRIS Università di Bologna (<https://cris.unibo.it/>)*

***When citing, please refer to the published version.***

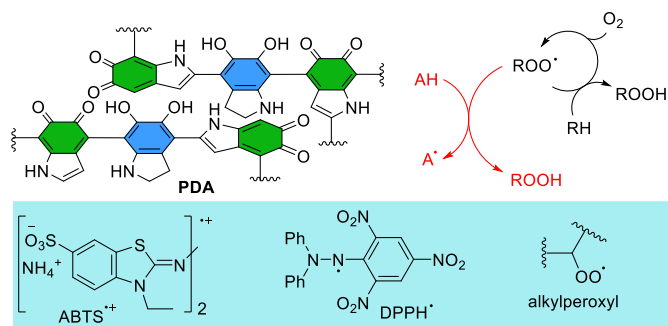
# Expanding the spectrum of polydopamine antioxidant activity by nitroxide conjugation

Fabio Mollica, Rosa Lucernati and Riccardo Amorati\*

Polydopamine (PDA) materials are important due to their unique physicochemical properties and their potential as chemopreventive agents for diseases connected with oxidative stress. Although PDA has been suggested to have antioxidant activity, its efficacy is controversial and its mechanism of action is still unclear. Herein, we report that accurately purified PDA nanoparticles in water at pH 7.4 are unable to quench alkylperoxyls ( $\text{ROO}^\bullet$ ), that are the radicals responsible for the propagation of lipid peroxidation, despite PDA reacts with the model  $\text{DPPH}^\bullet$  and  $\text{ABTS}^{+\bullet}$  radicals. PDA nanoparticles prepared by copolymerization of dopamine with the dialkyl nitroxide 4-NH<sub>2</sub>TEMPO show instead good antioxidant activity, thanks to the  $\text{ROO}^\bullet$  trapping ability of the nitroxide. Theoretical calculations performed on a quinone-catechol dimer, reproducing the structural motive of PDA, indicate a reactivity with  $\text{ROO}^\bullet$  similar to catechol. These results suggest that PDA nanoparticles have an “onion-like” structure, with catechol rich core and a surface mainly represented by quinones. The importance of assessing the antioxidant activity by inhibited autoxidation studies is also discussed.

## Introduction

Melanins are a family of pigments formed by the oxidative polymerization of biologically-occurring phenols, including tyrosine, DOPA and dopamine (DA).<sup>1,2</sup> Polydopamine (PDA) has recently attracted enormous interest because of its excellent adhesion properties, redox activity and its ability to easily form films and nanoparticles.<sup>3</sup> Although the exact molecular structure of PDA is still debated, there are evidences that it mainly consists of *ortho*-benzoquinone and 1,2-dihydroxyphenol (catechol) units, held together by both covalent and non-covalent interactions (Scheme 1).<sup>4</sup> The mechanism of the antioxidant activity of PDA has been object of many studies, recently reviewed,<sup>5</sup> but it is far from being clarified.<sup>5</sup> PDA has been reported to trap free radicals such as  $\text{HO}^\bullet$ ,  $\text{NO}^\bullet$ , 2,2-diphenyl-1-picrylhydrazyl ( $\text{DPPH}^\bullet$ ) and the 2,2'-azino-bis(3-ethylbenzthiazoline-6-sulfonic acid) radical cation ( $\text{ABTS}^{+\bullet}$ ) and to display superoxide-dismutase activity.<sup>5,6,7</sup> Very little is known about the reactivity of PDA toward peroxyl radicals that are the kinetically relevant oxidizing species that propagate lipid peroxidation (Scheme 1).<sup>8,9,10</sup> In a recent communication, we have shown that, in acetonitrile, PDA does not react with alkylperoxyl radicals ( $\text{ROO}^\bullet$ ) and thus it is unable to stop the lipid peroxidation of a model substrate. Instead, we could observe antioxidant activity only in the presence of both  $\text{ROO}^\bullet$  and  $\text{HOO}^\bullet$  radicals.<sup>11</sup> The role of the solvent on these reactions



**Scheme 1.** PDA structure, mechanism of action of radical trapping antioxidants and structure of peroxyl and model radicals.

and the reason why PDA is reactive with  $\text{DPPH}^\bullet$  and  $\text{ABTS}^{+\bullet}$  radicals but not with  $\text{ROO}^\bullet$  remain unclear. Moreover, as the antioxidant activity of PDA is expected to be influenced by the release of low molecular weight monomers or oligomers from the polymer, also the influence of PDA purification should be better clarified. Herein, we aim at expanding the knowledge on the antioxidant activity of PDA by measuring the reaction of PDA nanoparticles with biologically relevant  $\text{ROO}^\bullet$  radicals in water at pH 7.4, and by comparing the results to those obtained with  $\text{DPPH}^\bullet$  and  $\text{ABTS}^{+\bullet}$  (Scheme 1) that are the two most popular radicals used in *in-vitro* antioxidant activity assays. We also envisaged to increase the antioxidant activity of PDA by introducing a dialkyl nitroxide into the polymer, as this kind of strategy was shown to increase the protection from radiations of keratinocytes by PDA.<sup>12</sup> TEMPO (2,2,6,6-tetramethylpiperidinoxyl)-derived nitroxides in fact are very active  $\text{ROO}^\bullet$  quenchers in water and they show catalytic activity thanks to their ability to switch between the oxoammonium

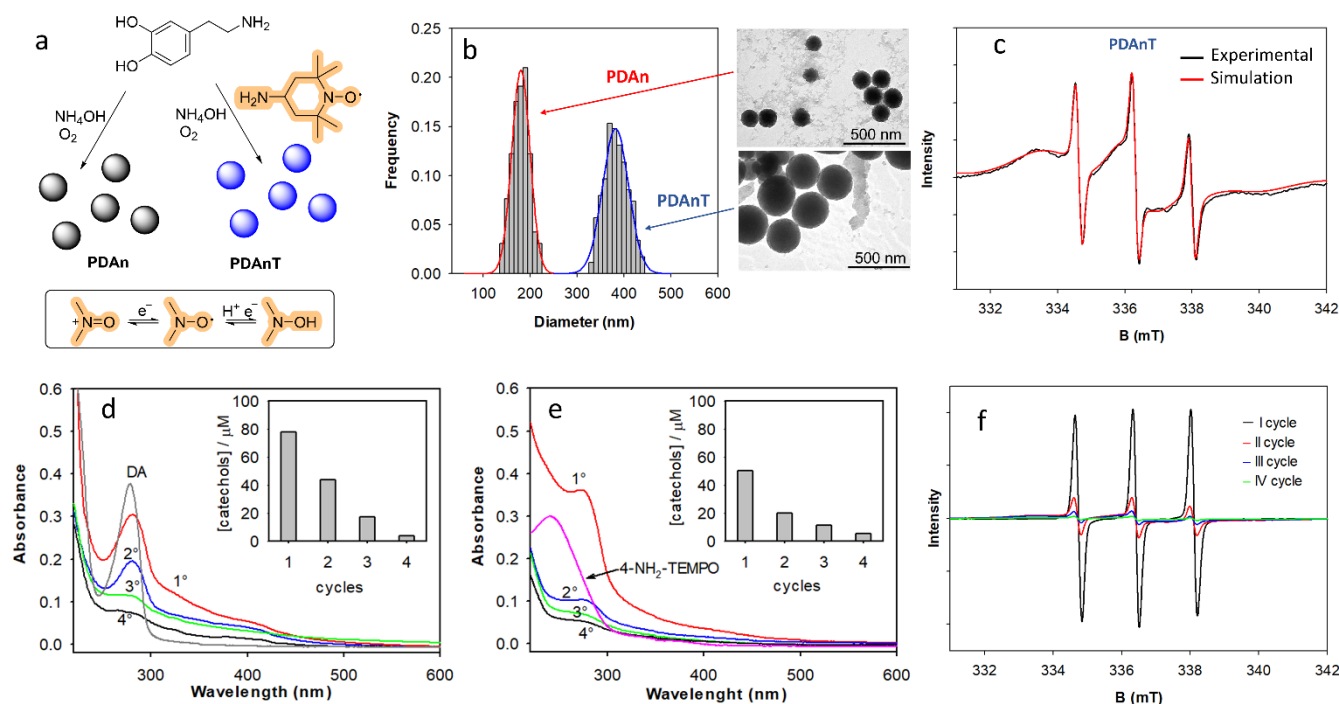


**Figure 1.** a) Synthesis and redox properties of nitroxides; b) TEM images of PDAn and PDAnT; c) experimental and simulated EPR spectrum of PDAnT in water (0.9 mg/mL); d,e) UV-vis spectra of the dialysates after each dialysis cycle for PDAn (d) and PDAnT (e), the insets show the concentration of catechol impurities; f) EPR spectra of the dialysates of PDAnT.

( $\text{N}=\text{O}^+$ ) and hydroxylamine (NOH) forms (Figure 1a).<sup>13,14,15</sup> We therefore linked 4-NH<sub>2</sub>TEMPO (4-amino-2,2,6,6-tetramethylpiperidinoxyl radical) to PDA by an original copolymerization strategy (Figure 2a). The effect of the purification procedure on the radical trapping ability of PDA and the implication of these results on PDA antioxidant activity are discussed.

## Results

### Synthesis and characterization

Polydopamine nanoparticles (PDAn) were synthesized by oxidative polymerization of DA under air, by mixing DA (as hydrochloride) and NH<sub>4</sub>OH, following an already reported procedure (Figure 1a).<sup>16,17</sup> Polydopamine / 4-NH<sub>2</sub>TEMPO nanoparticles (PDAnT) were synthesized by oxidative DA polymerization in the presence of 4-NH<sub>2</sub>TEMPO, after an accurate choice of the DA / 4-NH<sub>2</sub>TEMPO ratio. We found that 4-NH<sub>2</sub>TEMPO caused a fast oxidation of DA, yielding a polydisperse material, in agreement with previous reports on 2-phenyl-4,4,5,5-tetramethylimidazoline-1-oxyl 3-oxide (PTIO\*) effect on DA polymerization.<sup>18</sup> EPR analysis of the DA / 4-NH<sub>2</sub>TEMPO reaction showed that the signal of 4-NH<sub>2</sub>TEMPO disappeared in a few minutes, then it formed again after the addition of NH<sub>4</sub>OH, suggesting that the nitroxide is first reduced to hydroxylamine by DA, then it is oxidized back to nitroxide by O<sub>2</sub> (see Figure S1). Infrared (IR) and UV-vis spectra showed the typical features of polydopamine,<sup>16</sup> and transmission electron microscopy (TEM) and dynamic light scattering (DLS) analysis indicated that both materials were reasonably monodisperse. TEM diameters were 180 and 380 for PDAn and PDAnT

respectively, and were in agreement with DLS determinations (Figure 1b and Figure S2-S4).

**EPR characterization.** X-band Electron paramagnetic resonance (EPR) spectra of PDAn showed a weak signal, attributed to a semiquinone radical formed by the comproportionation of catechol and quinone groups,<sup>19</sup> whose concentration was 6.6  $\mu\text{mol/g}$ , in agreement with previous reports.<sup>12,19</sup> In the case of PDAnT an intense spectrum typical of a nitroxide in the slow-motion regime, characterized by broadened lines with uneven height,<sup>15</sup> was detected (Figure 1c). This EPR spectrum was successfully interpreted by numerical fitting by the EasySpin software (see Figure 1c), revealing the presence of about 97% 4-NH<sub>2</sub>TEMPO tightly bound to the nanoparticle, and 3% of “fast moving” nitroxide (see Figures S5-S7 for details).<sup>20</sup> The spin concentration in PDAnT was 190  $\mu\text{mol/g}$ . The spectral features and the spin concentration of PDAnT were comparable to those reported by Gianneschi and co-workers for polydopamine nanoparticles bearing covalently bound TEMPO residues (reported spin densities ranged from 101 to 379  $\mu\text{mol/g}$  depending on the preparation procedure).<sup>12</sup>

**Purification of PDA nanoparticles.** All nanoparticles were purified by three centrifugation cycles at 11500 g and one at 1500 g to separate the bigger aggregates, followed by four overnight dialysis cycles in deionized water. Dialysis did not significantly change the dimensions and the spectral features of the nanoparticles (see Figures S2-S3). The dialysate liquids were collected and concentrated under reduced pressure. UV-vis analysis, reported in Figure 1d-e, showed the presence of an absorption peak at 280 nm which was attributed to catechol impurities, given the similarity to the  $\lambda_{\text{max}}$  of DA (278 nm). The absorption between 400 and 500 nm suggested that also quinones were present. A more precise identification by electrospray ionization mass spectrometry (ESI-MS) was

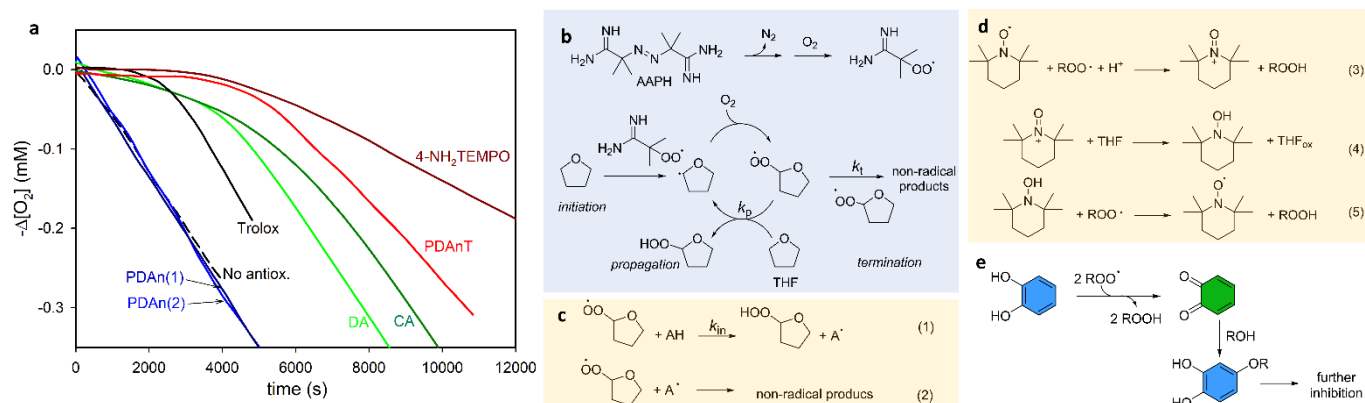


**Figure 2.** a) Oxygen consumption during the autoxidation of THF (1.2 M) initiated by AAPH (50 mM) at 30 °C, pH 7.4, in the presence of: PDAn purified by centrifugation (PDAn(1)) or by both centrifugation and dialysis (PDAn(2)) (20 μg/mL); Trolox (38 μM); DA (25 μM); CA (25 μM); PDAnT (22 μg/mL); 4-NH<sub>2</sub>TEMPO (25 μM). b) kinetic scheme of THF autoxidation. c) inhibition of autoxidation by a generic chain-breaking antioxidant AH. d) catalytic inhibition of autoxidation by nitroxides. e) solvent (ROH) addition to *ortho*-quinones derived from catechols increase the duration of inhibition.

unsuccessful, although it excluded the presence of unreacted DA or of catechols deriving from DA cyclization (i.e. 5,6-dihydroxyindole) and revealed the presence of signals presumably originating by the fragmentation of DA dimers or trimers (see Figure S8).<sup>4</sup> In the assumption that molar absorptivity of these impurities was the same as DA, their amount in the samples ranged from 78 to 4 μM, and diminished through the dialysis cycles (see the insets of Figure 1d-e). In the case of PDAnT, beside the presence of catechol impurities, the UV-vis spectra also showed the occurrence of unreacted 4-NH<sub>2</sub>TEMPO (purple line in Fig 1e). The residual 4-NH<sub>2</sub>TEMPO could be better quantified by EPR spectroscopy, and it showed a decrease from 45 to 0.8 μM after 4 dialysis cycles (Figure 1f). It should be emphasized that the spectrum of 4-NH<sub>2</sub>TEMPO free in solution is markedly different from that of PDAnT thus providing a clear proof of the linkage of the nitroxide to the nanoparticle, and an easy measure of the degree of purification of the material.

### Reaction with peroxy radicals

The ability to trap alkylperoxy (ROO<sup>•</sup>) radicals in water was measured by studying the inhibition of the autoxidation of tetrahydrofuran (THF)<sup>21</sup> as described in Figure 2. The reaction was initiated by the decomposition of the thermal azoinitiator 2,2'-azobis(2-amidinopropane) dihydrochloride (AAPH) at 30 °C (Figure 2b) and the rate was determined by measuring the O<sub>2</sub> consumption with an automatic gas-uptake recording apparatus.<sup>21</sup> In the absence of antioxidants, O<sub>2</sub> decreased linearly (see dashed line in Figure 2a) while in the presence of antioxidants the O<sub>2</sub> consumption was reduced, and an inhibition period was observed. The typical reactions of phenolic antioxidants with ROO<sup>•</sup> radicals are shown by equations 1 and 2 in Figure 2c. From the slope of O<sub>2</sub> consumption and the length of the inhibition period, the inhibition constant  $k_{inh}$  and the number of radical trapped by the antioxidant (stoichiometric coefficient,  $n$ ) could be obtained (see experimental section).<sup>22</sup>

**Table 1.** Radical trapping stoichiometries measured in the different assays. Results are expressed as mol (or μmol) of radicals quenched by a mol or by a mg of antioxidant.

	mol <sub>rad</sub> /mol <sub>antiox</sub> <sup>a</sup>			μmol <sub>rad</sub> /mg <sub>antiox</sub> <sup>b</sup>	
	ROO <sup>•</sup>	DPPH <sup>•</sup>	ABTS <sup>•+</sup>	DPPH <sup>•</sup>	ABTS <sup>•+</sup>
Dopamine	5.2±0.3	4.6±0.8	2.6±0.4	30±6	17±2
Catechol	6.1±0.3	-	-	-	-
4-NH <sub>2</sub> TEMPO	5.0±0.3	≈0	≈0	≈0	≈0
PDAnT	2.0±0.3 <sup>c</sup>	-	-	5.1±0.9	2.0±0.4
PDAn	≈0	-	-	6.5±0.2	4.3±0.8

a) moles of radicals quenched by a mole of antioxidant; b) μmoles of radicals quenched by a mg of antioxidant; c) referred to the nitroxide concentration, determined by EPR.

The results showed that DA and catechol (CA), used for comparison purposes, had a high antioxidant activity, whereas PDAn was unable to slow down the THF autoxidation. Interestingly, PDAn samples before and after the purification by dialysis were both inactive, indicating that the concentration of catechol impurities was too low to influence THF autoxidation. To better clarify the role of impurities, we performed the same experiment on a sample of PDAn purified only by one cycle of centrifugation. In this case, THF autoxidation was inhibited (see Figure S9), thus confirming that insufficient purification leads to an overestimation of the antioxidant activity. The experiments performed with 4-NH<sub>2</sub>TEMPO confirmed the previous finding<sup>15</sup> that this nitroxide is an excellent quencher of ROO<sup>•</sup> and, gratifyingly, also PDAnT displayed a similar strong antioxidant activity. The antioxidant activity in water of nitroxides is due to the electron transfer from R<sub>2</sub>N-O<sup>•</sup> moiety to ROO<sup>•</sup> to form the oxoammonium cation (R<sub>2</sub>N=O<sup>+</sup>) and ROO<sup>-</sup>, which is protonated by the solvent to afford ROOH (Figure 2d reaction 3). The nitroxide is then regenerated by the reaction of R<sub>2</sub>N=O<sup>+</sup> with reductants (such as THF) to afford the hydroxylamine, that in turn reacts with ROO<sup>•</sup> and regenerates the nitroxide (Figure 2d, reactions 4 and 5).<sup>13,14,15</sup> Except for PDAn, for all investigated compounds a very strong inhibition of THF autoxidation was

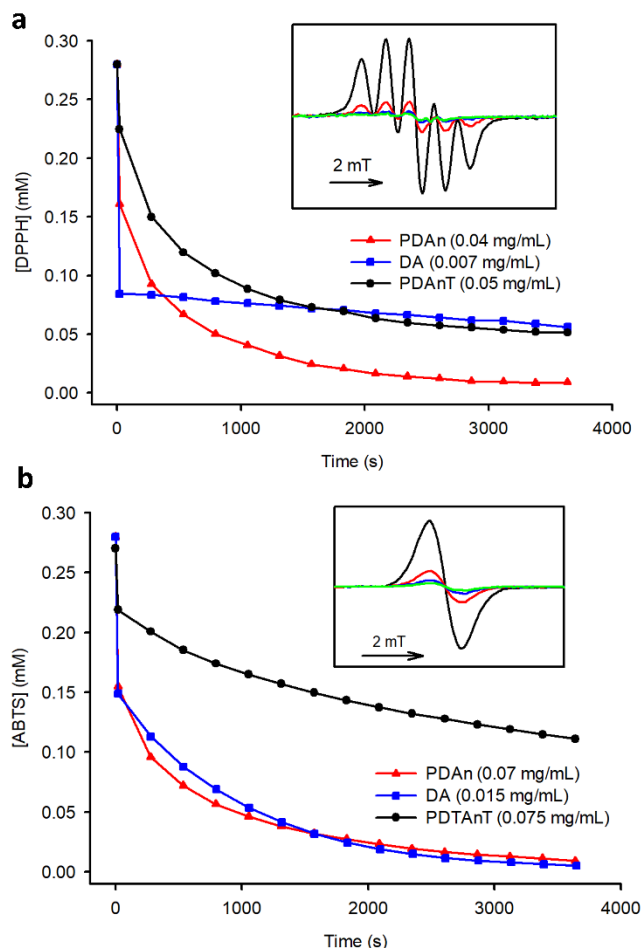


**Figure 3.** Reaction with DPPH, solvent ethanol (a), and with ABTS, solvent water (b). The insets show the decay of EPR spectra of the two radicals (time interval 15 min).

observed, implying that  $k_{inh}$  values were bigger than  $5 \times 10^5 \text{ M}^{-1} \text{ s}^{-1}$ . The stoichiometries of the antioxidants, obtained from the duration of the antioxidant effect, are reported in Table 1. The large stoichiometries of DA and CA compared to that of the reference antioxidant Trolox, can be ascribed to the reactivity of the *ortho*-quinone with the solvent that regenerate the catechol moiety (Figure 2e).<sup>23,24</sup> If considering that a catechol group is able to donate two H-atoms to two  $\text{ROO}^\bullet$ , the stoichiometry of about 6 suggests that the catechol group is regenerated twice. In the case of nitroxides, the stoichiometry  $> 1$  is instead due to the catalytic cycle shown in reactions 3-5.

### Reaction with stable radicals

The reactions of PDA, PDAnT, DA and 4-NH<sub>2</sub>TEMPO with the stable radicals DPPH $^\bullet$  and ABTS $^{2+}$  were investigated by EPR spectroscopy to avoid interference by the intense color of polydopamine. The typical results of time course experiments are reported in Figure 3 and Figures S10-S17, and the stoichiometry of radical trapping after 45 min is summarized in Table 1. The results clearly show that polydopamine-based nanoparticles react with the two radicals, although less efficiently than the monomer DA. In the case of the reaction with DPPH $^\bullet$ , the reaction with DA occurred instantaneously during the mixing of the reactants, with a stoichiometry of 5.4 DPPH $^\bullet$  radicals trapped by each DA molecule. Even if used at

higher concentrations (on weight basis), the reactions of PDA and PDAnT were slower than that of DA, and the stoichiometries (on weight basis) were much smaller (see Table 1). 4-NH<sub>2</sub>TEMPO was completely inactive, in agreement with previous reports.<sup>25</sup>

### Reactivity of PDA models

To clarify the reasons for the lack of reactivity of PDA with  $\text{ROO}^\bullet$ , this reaction was investigated by means of theoretical calculations. In general, the reaction of catechol derivatives with  $\text{ROO}^\bullet$  can follow different proton, hydrogen and electron transfer pathways that are summarized in Table 2.<sup>26,27</sup> Undissociated catechols (**I**) can react with  $\text{ROO}^\bullet$  by H-atom transfer (path A) to afford the phenoxyl radical **II** that, at pH 7.4, dissociates to the radical anion **V** (the  $\text{pK}_a$  of *ortho*-semiquinone is 5.0).<sup>28</sup> Deprotonation of catechols (path B) affords the anion **III**, which can react with  $\text{ROO}^\bullet$  either via a H-atom transfer

**Table 2.** Theoretical calculation of the reaction of catechol derivatives and  $\text{ROO}^\bullet$ .

	$\Delta G^\ddagger(\text{A})$ kcal/mol	$\text{pK}_a(\text{B})$	$\Delta G^\circ(\text{C})$ kcal/mol	$\Delta G^\circ(\text{D})$ kcal/mol
 CA	11.3	9.1	-12.7	6.4
 DA	12.3	8.7	-11.8	9.7
 DHI	8.4	9.4	-14.8	0.15
 DHID	12.0	8.5	-13.2	3.5

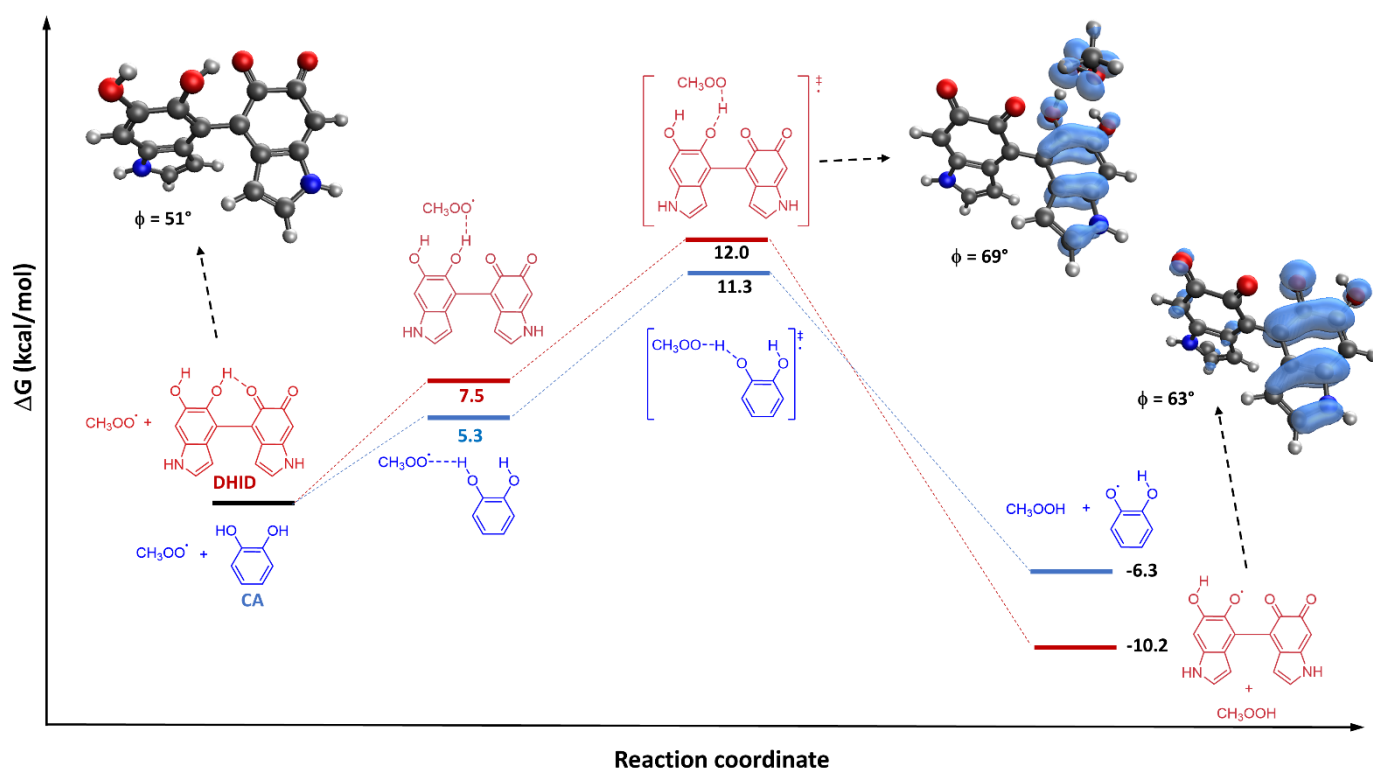


**Figure 4.** Free energy profile for H-atom abstraction from the DHID, model of the catechol moieties in PDA, and CA by a peroxy radical. The dihedral angle  $\phi$  between the aryl and the *ortho*-quinone rings is reported. Blue surfaces represent the spin density. Free-energy changes are calculated in water at 25 °C.

(path C) or via electron transfer (path D) followed by proton exchange between the reactants. The B+D reaction sequence is reminiscent of the SPLET (sequential proton loss electron transfer) mechanism often invoked to explain the reactivity of phenols with radicals.<sup>26</sup> The barrier of step A, the  $pK_a$  values (step B)<sup>29</sup> and the free energy variation for the steps C and D were investigated by means of DFT theoretical calculations.<sup>30</sup> This approach is aimed at obtaining a qualitative comparison between selected species relevant for polydopamine chemistry: DA, CA, 2,5-dihydroxyindole (DHI), and for a partially oxidized 4-4' dimer of 2,5-dihydroxyindole (DHID), whose structure is reported in Table 2 and Figure 4. The latter molecule was chosen as simplified model of PDAn to simulate the packing in the polymer,<sup>31</sup> as it is the most stable among the DHI dimers containing both the quinone and the catechol moiety in close proximity.<sup>32</sup>

The results, reported in Table 2 and Figure 4, show that the direct reaction of  $ROO^\bullet$  with all the investigated catechols (path A) has an energy barrier of about 12 kcal/mol, except in the case of DHI whose  $\Delta G^\ddagger$  is calculated as 8.4 kcal/mol. The lower barrier of DHI can be explained in terms of radical stabilization by the indole ring. Interestingly, DHID has similar  $\Delta G^\ddagger$  as CA, despite its reaction with  $CH_3OO^\bullet$  is overall more exergonic (see Figure 4). This result can be explained in terms of radical delocalization on the *ortho*-quinone ring (see the blue surfaces in Figure 4), which is dependent on the dihedral angle between the aryl and the *ortho*-quinone rings (angle  $\phi$  in Figure 4). The delocalization is highest when the two rings are on the same plane ( $\phi = 0$ ) and is minimal for the perpendicular orientation. Therefore, the bigger  $\phi$  in the transition state (TS) than in the

products calculated for DHID suggests a smaller radical stabilization in the TS.

Regarding the acidity of the investigated compounds (step B), the  $pK_a$  of DHID is smaller than that of CA, DA and DHI, suggesting that the dimer is able to form the anion more easily than the other catechols.

The path C is significantly exergonic for all compounds, with DHID having a slightly smaller  $\Delta G^\circ$  than CA and DA. The  $\Delta G^\ddagger$  values for step C could not be calculated because the reaction was barrierless.

The electron transfer step (path D) results endergonic or, only in the case of DHI, slightly exergonic, suggesting that SPLET mechanism plays a negligible role in the reactivity of catechols with  $ROO^\bullet$  in water. Overall, all the calculated descriptors strongly support the idea that DHID is less reactive than DHI, but it has a comparable reactivity toward  $ROO^\bullet$  than that of the catechols CA and DA which in water are good antioxidants (see Figure 2a).

## Discussion

### PDA purification.

The first point that needs to be clarified when addressing the antioxidant activity of PDA is the role of diffusible monomers and oligomers that may be absorbed into the material. It is well known that certain drugs and chemicals bind to natural and synthetic melanins and are retained in the pigments for long periods.<sup>33</sup> Drugs with aromatic and basic groups such as chloroquine, chlorpromazine and levofloxacin are tightly absorbed,<sup>34</sup> thus the entrapment of DA and of its monomeric

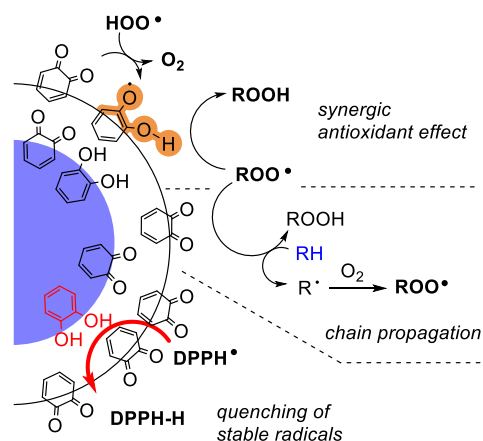


and oligomeric derivatives into the growing PD nanoparticles is not unexpected. As DA and its derivatives such as DHI are highly antioxidant,<sup>35</sup> their presence must be kept into account when studying PDA. Herein, the purification of PDA nanoparticles was performed in two steps, consisting in three centrifuge cycles followed by four overnight dialysis cycles. Moreover, at each dialysis cycles, the dialysate solutions were concentrated and analysed by UV-vis spectrometry. These experiments clearly showed that diffusible molecules, containing catechol and quinone groups, were present in the samples and that their concentration decreased somewhat slowly despite the purification efforts (see insets in Figure 1d-e), suggesting a release from PDAn and PDAnT. We ascertained the role of diffusible catechols by performing all the tests of the antioxidant activity before and after the dialysis cycles and we found no difference between the two samples. Apparently, the concentration of the impurities present after the three centrifugations was too low to contribute to the reaction with radicals. To better investigate this point, we also prepared a sample of PDAn purified only by a single centrifuge cycle, and we tested its ability to inhibit THF autoxidation. The result reported in Figure S7, showed a good antioxidant effect, thus indicating that insufficient purification may lead to false positive results. We believe that the same caution should be paid also when studying the antioxidant activity of phenolic polymers in general.

#### Intrinsic ROO• trapping activity of PDA

The study of the ability of PDAn to slow down the autoxidation of THF in water at pH 7.4 confirmed our previous results obtained in acetonitrile solution indicating that PDAn does not possess any direct chain-breaking antioxidant activity. While this result seems in contrast with the many claims of antioxidant activity of PDA, it is in agreement with a study of Nau and co-workers who found that sepia melanin is a poor quencher of the excited states of benzophenone and of 2,3-diazabicyclo[2.2.2]oct-2-ene, and has a nearly negligible antioxidant efficacy on liposome oxidation.<sup>36</sup> Antioxidant activity of PDA was instead evident when the autoxidation was initiated by light, because of its UV absorbing properties.<sup>37</sup> The lack of reactivity with ROO• radicals is puzzling if compared to the fact that PDA is able to quench both DPPH• and ABTS••. A possible explanation may be the presence of strong H-bond complexes between the catechol moieties and the carbonyl groups in PDA, which might increase the dissociation energy of the O-H group and impair the reaction with ROO•.<sup>38,39</sup> However, this hypothesis should be discharged because theoretical calculations indicate that DHID, even if its catechol groups is H-bonded to the carbonyl, has a reactivity with ROO• similar to DA or CA, suggesting that catechols of PDA should trap ROO• radicals similarly to DA and CA in water. Therefore, to explain the lack of antioxidant effect of PDAn, we hypothesise that PDAn surface is constituted only by *ortho*-quinone groups, while catechol moieties are confined in the inner core. This two-layer structure can be justified because, during the synthesis of PDAn, any catechol group exposed on the surface would be deprotonated and oxidized by O<sub>2</sub>. The radical quenching ability of PDAn can be rationalized by admitting that DPPH• and ABTS••

are able to reach the inner part of the nanoparticle by a relatively slow diffusion process and are quenched by the catechol groups, as shown in Scheme 2.



**Scheme 2.** Layered structure of polydopamine nanoparticles explaining the absence of direct reaction with ROO•, the synergistic antioxidant effect in the presence of HOO• and ROO• radicals, and the reactivity toward stable radicals such as DPPH•. RH represents the oxidizable substrate, that compete with polydopamine for the ROO• radical

In the case of ROO• radicals, this diffusion process must compete with the propagation of the oxidative chain, thus the efficacy of radical trapping is much diminished. The presence of a quinone-rich outer shell also explains why PDAn is a good trap for reducing radicals such as HOO• and O<sub>2</sub><sup>•-</sup> (see Scheme 2).<sup>3,11,40</sup> In this case, the radicals reduce the *ortho*-quinone moieties to the corresponding semiquinones, which in turn possess radical trapping capabilities toward oxidizing ROO• radicals.

#### Antioxidant activity of PDAnT

The idea of linking nitroxides to PDA was first sought by Woehlke et al. with the aim to obtain a redox active functional surface.<sup>41</sup> To incorporate a TEMPO moiety in PDA, they synthesized a precursor consisting in 4-NH<sub>2</sub>TEMPO covalently linked to 3,4-dihydroxy-L-phenylalanine (L-DOPA) by an amide bond. The same precursor was then adopted by Gianneschi and co-workers to obtain “radical enriched” PDA nanoparticles that displayed protective properties against reactive oxygen species in keratinocytes.<sup>12</sup> Herein, we achieved the same goal by using a straightforward one-pot strategy consisting in the oxidative copolymerization of 4-NH<sub>2</sub>TEMPO and DA in basic conditions. The link of TEMPO moieties to PDA is expected to be based on the nucleophilic attack of the amino group of 4-NH<sub>2</sub>TEMPO to the *ortho*-quinone groups of PDAn, similarly to other amines which have been reported to be incorporated in the growing PDA polymer (e.g. tris(hydroxymethyl)aminomethane).<sup>42</sup> In the search for the best synthetic strategy, we attempted different approaches, such as 4-NH<sub>2</sub>TEMPO addition to preformed PDAn in basic conditions, or the use of the non-radical TEMPO precursor 4-amino-2,2,6,6-tetramethylpiperidine, but these efforts proved unsuccessful. The shape of the EPR spectrum of PDAnT obtained after a thorough purification clearly indicated that nitroxides are bound to the nanoparticles. Despite its simplicity, our method provided PDAnT with an EPR spectrum and a radical enrichment that were very similar to those



reported by Gianneschi and co-workers.<sup>12</sup> Gratified by this result, we investigated the ROO<sup>•</sup> trapping ability of PDAnT as this piece of information is important to rationalize the biological activity of this and of analogous materials previously reported. The inhibition of THF autooxidation in water was very strong and was similar to that observed in the case of the parent 4-NH<sub>2</sub>TEMPO. The stoichiometry of radicals trapped by PDAnT suggests that, although a significant part of TEMPO moieties is available to the reaction with ROO<sup>•</sup>, another portion (about 60%) is buried into the polymer and is therefore inactive.

## Conclusions

In this work we have shown that polydopamine nanoparticles (PDAn) in water are not able to directly trap alkyl peroxy radicals (ROO<sup>•</sup>), that are responsible of chain propagation in the autooxidation of organic substrates. Instead, PDAn can quench the DPPH<sup>•</sup> and ABTS<sup>•+</sup> stable radicals.<sup>43,44</sup> Together with our previous results indicating that PDAn reacts with the reducing HOO<sup>•</sup> radicals, this demonstrates that the surface of PDAn is mainly constituted by *ortho*-quinones which are unable to trap ROO<sup>•</sup> radicals but can interact with the reducing superoxide radical (HOO<sup>•</sup> / O<sub>2</sub><sup>•-</sup>), resulting in an antioxidant effect. On the other hand, the slow reaction with DPPH<sup>•</sup> and ABTS<sup>•+</sup> can be explained by considering that catechol moieties are present in the inner core of PDAn, where they cannot be promptly accessed by ROO<sup>•</sup> and thus cannot compete with chain propagation. We have also shown that PDAn loaded with a stable nitroxide of the TEMPO family, PDAnT, are excellent antioxidants and show a high reactivity toward ROO<sup>•</sup>. As nitroxide-containing PDA nanoparticles have been shown to have low toxicity in cells,<sup>12</sup> our findings further reinforce the idea that nitroxide-decorated PDA nanoparticles are promising platforms for the development of novel and more effective antioxidant materials for biomedical and food applications. Our results also provide evidence that DPPH<sup>•</sup> and ABTS<sup>•+</sup> should be used with caution to predict the reaction with ROO<sup>•</sup>, as these assays are prone to false positive or negative results due to their structural difference with the biologically relevant alkylperoxy radicals.<sup>45</sup>

## Experimental section

### Materials and methods

Analytical-grade solvents and commercially available reagents were of the highest purity commercially available and were used as received, unless otherwise stated. THF was purified by distillation, water was Millipore grade (resistivity  $\geq 18$  M $\Omega$ ). The radical ABTS<sup>•+</sup> was prepared by mixing a 7 mM aqueous solution of 2,2'-Azino-bis (3-ethylbenzothiazolin-6-sulfonic) ammonium salt with a 2.45 mM potassium persulfate solution and stored overnight in the dark.<sup>46</sup> Its concentration was determined by EPR using DPPH<sup>•</sup> solution 0.28 mM as standard.

**Transmission electron microscopy (TEM) measurements.** A Philips CM 100 TEM operating at 80 kV was used. For TEM investigations, a few drops of NPs solution in water was deposited on Formvar copper grids and dried under high vacuum.

**Dynamic light scattering measurements (DLS).** The determination of the NPs hydrodynamic diameter distributions was carried out through Dynamic Light Scattering measurements employing a Malvern Nano ZS instrument equipped with a 633 nm laser diode. Samples were housed in disposable polystyrene cuvettes of 1 cm optical path length, using water as solvent.

**IR spectra.** Infrared absorption spectra were directly recorded on solids on a Perkin-Elmer Spectrum 100 FT-IR Spectrometer equipped with a universal ATR (attenuated total reflectance) accessory (contact crystal: diamond).

**EPR spectroscopy studies.** The electron paramagnetic resonance (EPR) spectra were collected at 35 °C with a MiniScope MS 5000 (Magnettech) in glass capillary tubes. The concentration of nitroxide bound to the nanoparticles was determined by comparing the double integral of its EPR spectrum to that of 4-NH<sub>2</sub>TEMPO. Spectra simulation was performed by the software EasySpin with the graphical interface SimLabel as shown in Figures S4-6.<sup>20,47</sup>

### Synthesis

**PDAn.** The synthesis was carried out by oxidative polymerization of DA at basic pH.<sup>16,17</sup> Dopamine-HCl (130 mg, 11 mM) was solubilized in a mixture of deionized water (51 mL) and ethanol (9 mL) and was heated to 50 °C under stirring. Then 275  $\mu$ L of 30% NH<sub>4</sub>OH were added (0.24 M) and the solution turned from a pale yellow to a dark brown color in a few minutes. The reaction was left under stirring for 24 hours at 50 °C. The obtained PDA nanoparticles (PDAn) were purified by three high-speed centrifugation cycles (11500 g for 15 minutes, washing the precipitate each time with deionized water) followed by one low-speed centrifugation (1500 g for 10 minutes) to eliminate the bigger aggregates. An aliquot of PDAn was further purified using a dialysis membrane (Cut-off = 14 kDa) and 500 mL of deionized water, for a total of four cycles. To monitor purification, at each dialysis cycle, 30 mL of dialysate water was collected and concentrated, and was analyzed by UV-Vis spectra and ESI-MS (see Figure S8 for details). Known volumes of PDAn at different levels of purification were lyophilized to obtain their concentration, which were 0.78 mg/mL and 0.82 mg/mL for PDAn purified only by centrifugation or by centrifugation and dialysis, respectively. The nanoparticles were characterized by DLS, TEM, UV-Vis spectroscopy and ATR FT-IR as reported in Figures 1 and S2.

**PDAnT.** After several tests, the synthesis procedure was modified to slow down the polymerization, to obtain functionalized, monodisperse nanoparticles. In a flask dopamine-HCl (30 mg, 11 mM) was solubilized in deionized water (12 mL) and stirred and heated to 50°C. In another vessel, NH<sub>2</sub>-TEMPO (18 mg, 7.5 mM), 30% NH<sub>4</sub>OH (63 mL, 0.11 M), and ethanol (2 mL) were mixed and added slowly to the dopamine solution and were left to react for 24 hours at 50 °C. The final product was purified and characterized as previously described for PDAn (see Figures S3) and its concentration was 0.9 mg/mL.

**Reaction with DPPH<sup>•</sup> and ABTS<sup>•+</sup> radicals.** A stock solution of the stable radical was mixed to different amounts of concentrated solution of the investigated phenols or nanoparticles. After mixing for about three seconds, the reaction mixture was loaded in a 50 mL glass capillary tube and

introduced into the EPR cavity thermostatted at 37 °C. Spectra were collected every 4 minutes.

**Autoxidation studies.** The kinetics of reaction with alkylperoxy radicals was studied by autoxidation experiments in a differential oxygen-uptake apparatus based on a Validyne DP 15 pressure transducer built in our laboratory.<sup>48</sup> The samples consisted of AAPH (50 mM), THF (10 % v/v, 1.2 M), pH 7.4 phosphate buffer 0.1 M (temperature = 30 °C) under vigorous stirring. By using the  $\alpha$ -tocopherol hydrosoluble analogue Trolox as a reference antioxidant (having  $n=2$ ), the rate of radical initiation was calculated by the relation  $R_i = n[\text{Antiox.}]/\tau$ , where  $\tau$  is the duration of the inhibited period, as  $R_i = 3.0 \times 10^{-8} \text{ Ms}^{-1}$ . This equation also provided the stoichiometry  $n$  of the antioxidant (see Table 1).<sup>48</sup>

### Theoretical calculations

Geometry optimization and frequencies were computed at the B3LYP/6-311+G(d,p) level by using Gaussian 09.<sup>49</sup> The solvent was modelled by the standard self-consistent reaction field (PCM) procedure as implemented in the Gaussian 09 set of programs. Stationary points were confirmed by checking the absence of imaginary frequencies. The  $pK_a$  values were calculated by following the empirical relationship proposed by Galano et al.<sup>29</sup> by using Equation 6 where  $\Delta G_{S(BA)}$  represents the difference in Gibbs free energy (in kcal/mol), in aqueous solution, between the acid (A) and its corresponding conjugated base (B).

$$pK_a = m \Delta G_{S(BA)} + C_0 \quad (6)$$

The empirical parameters  $m$  and  $C_0$  were 0.286 and  $-73.092$  respectively, that have been optimized for the deprotonation of phenolic OH groups at the theory level of B3LYP/6-311++g(d,p) SCRF=(SMD,Solvent=Water).

### Author Contributions

Investigation and data curation were performed by R. L and F. M. Conceptualization, funding acquisition, writing (original draft, review & editing) were performed by R. A.

### Conflicts of interest

There are no conflicts to declare.

### Acknowledgements

F.M. gratefully acknowledges a fellowship from ENI SpA. We thank Dr. Maria Roberta Randi for technical assistance in TEM experiments and Paolo Amorati for the artwork used as the graphical abstract. The Department of Chemistry “G. Ciamician” acknowledges the Fondazione CarisBo for the funding of the project#18668 “Tecnologie avanzate per il controllo e lo sviluppo di molecole innovative per la salute”.

### References

- 1 M. d’Ischia, A. Napolitano, A. Pezzella, P. Meredith and M. Buehler. *Angew. Chem. Int. Ed.* 2020, **59**, 11196.
- 2 W. Cao, X. Zhou, N. C. Mc Callum, Z. Hu, Q. Z. Ni, U. Kapoor, C. M. Heil, K. S. Cay, T. Zand, A. J. Mantanona, A. Jayaraman, A. Dhinojwala, D. D. Deheyn, M. D. Shawkey, M. D. Burkart, J. D. Rinehart and N. C. Gianneschi. *J. Am. Chem. Soc.* 2021, **143**, 2622.
- 3 W. Cheng, X. Zeng, H. Chen, Z. Li, W. Zeng, L. Mei and Y. Zhao. *ACS Nano*, 2019, **13**, 8537.
- 4 Q. Lyu, N. Hsueh and C. L. L. Chai. *Polym. Chem.*, 2019, **10**, 5771.
- 5 J. Hu, L. Yang, P. Yang, S. Jiang, X. Liu and Y. Li. *Biomater. Sci.*, 2020, **8**, 4940.
- 6 L. Panzella, G. Gentile, G. D’Errico, N. F. Della Vecchia, M. E. Errico, A. Napolitano, C. Carfagna and M. d’Ischia. *Angew. Chem. Int. Ed.* 2013, **52**, 12684.
- 7 S. El Yakhlifi, M.-L. Alfieri, Y. Arntz, M. Eredia, A. Ciesielski, P. Samori, M. d’Ischia, V. Ball. *Colloids Surf. A: Physicochem. Eng. Asp.*, 2021, **614**, 126134.
- 8 M. C. Foti. *J. Agric. Food Chem.* 2015, **63**, 8765.
- 9 R. Amorati and L. Valgimigli. *Free Radic. Res.* 2015, **49**, 633.
- 10 R. Shah, L. A. Farmer, O. Zilka, A. T. M. Van Kessel and D. A. Pratt. *Cell Chem. Biol.* 2019, **26**, 1.
- 11 Y. Guo, A. Baschieri, F. Mollica, L. Valgimigli, J. Cedrowski, G. Litwinienko and R. Amorati. *Angew. Chem. Int. Ed.* 2021, **60**, 15220.
- 12 W. Cao, A. J. Mantanona, H. Mao, N. C. McCallum, Y. Jiao, C. Battistella, V. Caponetti, N. Zang, M. P. Thompson, M. Montalti, J. F. Stoddart, M. R. Wasielewski, J. D. Rinehart and N. C. Gianneschi. *Chem. Mater.* 2020, **32**, 5759.
- 13 M. Griesser, R. Shah, A. T. Van Kessel, O. Zilka, E. A. Haidasz, and D. A. Pratt. *J. Am. Chem. Soc.* 2018, **140**, 3798.
- 14 A. Baschieri, L. Valgimigli, S. Gabbanini, G. A. DiLabio, E. Romero-Montalvo and R. Amorati. *J. Am. Chem. Soc.* 2018, **140**, 10354.
- 15 D. Genovese, A. Baschieri, D. Vona, R. E. Baboi, F. Mollica, L. Prodi, R. Amorati and N. Zaccheroni. *ACS Appl. Mater. Interfaces* 2021, **13**, 31996.
- 16 Y. Huang, Y. Li, Z. Hu, X. Yue, M. T. Proetto, Y. Jones and N. C. Gianneschi. *ACS Cent. Sci.* 2017, **3**, 564.
- 17 X. Jiang, Y. Wang and M. Li. *Sci. Rep.* 2015, **4**, 6070.
- 18 X. Wang, Z. Chen, P. Yang, J. Hu, Z. Wang and Y. Li. *Polym. Chem.*, 2019, **10**, 4194.
- 19 K. Tadyszak, R. Mrówczyński and R. Carmieli. *J. Phys. Chem. B* 2021, **125**, 841.
- 20 S. Stoll and A. Schweiger. *J. Magn. Reson.* 2006, **178**, 42.
- 21 R. Amorati, A. Baschieri, G. Morroni, R. Gambino and L. Valgimigli. *Chem. Eur. J.* 2016, **22**, 7924.
- 22 R. Shah, J.-F. Poon, E. A. Haidasz and D. A. Pratt. *J. Org. Chem.* 2021, **86**, 6538.
- 23 S. Saito, H. Gao and J. Kawabata. *Helv. Chim. Acta*, 2006, **89**, 821.
- 24 S. Guernelli, A. Cariola, A. Baschieri, R. Amorati and P. Lo Meo. *Mater. Adv.*, 2020, **1**, 2501.
- 25 M. Pichla, G. Bartosz, N. Pieńkowska, I. Sadowska-Bartoszyńska. *Anal. Biochem.* 2020, **597**, 113698.
- 26 G. Litwinienko and K. U. Ingold. *Acc. Chem. Res.* 2007, **40**, 222.
- 27 R. Amorati, G. F. Pedulli, L. Cabrini, L. Zamboni and L. Landi. *J. Agric. Food Chem.* 2006, **54**, 8, 2932.
- 28 J. J. Warren, T. A. Tronic and J. M. Mayer. *Chem. Rev.* 2010, **110**, 6961.
- 29 A. Galano, A. Pérez-González, R. Castañeda-Arriaga, L. Muñoz-Rugeles, G. Mendoza-Sarmiento, A. Romero-Silva, A. Ibarra-Escutia, A. M. Rebollar-Zepeda, J. R. León-Carmona, M. A. Hernández-Olivares and J. R. Alvarez-Idaboy. *J. Chem. Inf. Model.* 2016, **56**, 1714.
- 30 A. Baschieri, L. Pulvirenti, V. Muccilli, R. Amorati and C. Tringali. *Org. Biomol. Chem.*, 2017, **15**, 6177.

- 31 J. Liebscher, R. Mrówczyński, H. A. Scheidt, C. Filip, N. D. Hädäde, R. Turcu, A. Bende and S. Beck. *Langmuir* 2013, **29**, 10539.
- 32 C.-T. Chen, F. J. Martin-Martinez, G. S. Jung and M. J. Buehler *Chem. Sci.*, 2017, **8**, 1631.
- 33 O. Karlsson and N. G. Lindquist. *Arch. Toxicol.* 2016, **90**, 1883.
- 34 P. Jakubiak, F. Lack, J. Thun, A. Urtti and R. Alvarez-Sánchez. *Mol. Pharmaceutics*, 2019, **16**, 2549.
- 35 S. Memoli, A. Napolitano, M. d'Ischia, G. Misuraca, A. Palumbo and G. Prota. *Biochim. Biophys. Acta* 1997, **1346**, 61.
- 36 X. Zhang, C. Erb, J. Flammer and W. M. Nau. *Photochem. Photobiol.*, 2000, **71**, 524.
- 37 A. Ezzahir. *J. Photochem. Photobiol. B: Biology*. 1989, **3**, 341.
- 38 R. Amorati, S. Menichetti, C. Viglianisi and M. C. Foti. *Chem. Commun.*, 2012, **48**, 11904.
- 39 M. C. Foti, L. R. C. Barclay and K. U. Ingold. *J. Am. Chem. Soc.* 2002, **124**, 12881.
- 40 A. Baschieri, R. Amorati, L. Valgimigli and L. Sambri. *J. Org. Chem.* 2019, **84**, 13655.
- 41 H. Woehlk, J. Steinkoenig, C. Lang, L. Michalek, V. Trouillet, P. Krolla, A. S. Goldmann, L. Barner, J. P. Blinco, C. Barner-Kowollik and K. E. Fairfull-Smith. *Langmuir*, 2018, **34**, 3264.
- 42 N. F. Della Vecchia, A.O Luchini, A. Napolitano, G. D'Errico, G. Vitiello, N. Szekely, M. d'Ischia and L. Paduano. *Langmuir* 2014, **30**, 9811.
- 43 H. Liu, X. Qu, H. Tan, J. Song, M. Lei, E. Kim, G. F. Payne and C. Liu *Acta Biomaterialia* 2019, **88**, 181-196.
- 44 Y. Jing, Z. Deng, X. Yang, L. Li, Y. Gao and W. Li *Chem. Commun.*, 2020, **56**, 10875-10878.
- 45 A. Baschieri and R. Amorati *Antioxidants*, 2021, **10**, 1551.
- 46 R. Re, N. Pellegrini, A. Proteggente, A. Pannala, M. Yang and C. Rice-Evans. *Free Radic. Biol. Med.* 1999, **26**, 1231.
- 47 E. Etienne, N. Le Breton, M. Martinho, E. Mileo and V. Belle, *Magn. Reson. Chem.* 2017, **55**, 714.
- 48 A. Baschieri, R. Amorati, T. Benelli, L. Mazzocchetti, E. D'Angelo and L. Valgimigli. *Antioxidants* 2019, **8**, 30.
- 49 Gaussian 09, Revision D.01, M. J. Frisch, G. W. Trucks, H. B. Schlegel, G. E. Scuseria, M. A. Robb, J. R. Cheeseman, G. Scalmani, V. Barone, B. Mennucci, G. A. Petersson, H. Nakatsuji, M. Caricato, X. Li, H. P. Hratchian, A. F. Izmaylov, J. Bloino, G. Zheng, J. L. Sonnenberg, M. Hada, M. Ehara, K. Toyota, R. Fukuda, J. Hasegawa, M. Ishida, T. Nakajima, Y. Honda, O. Kitao, H. Nakai, T. Vreven, J. A. Montgomery, Jr. , J. E. Peralta, F. Ogliaro, M. Bearpark, J. J. Heyd, E. Brothers, K. N. Kudin, V. N. Staroverov, R. Kobayashi, J. Normand, K. Raghavachari, A. Rendell, J. C. Burant, S. S. Iyengar, J. Tomasi, M. Cossi, N. Rega, J. M. Millam, M. Klene, J. E. Knox, J. B. Cross, V. Bakken, C. Adamo, J. Jaramillo, R. Gomperts, R. E. Stratmann, O. Yazyev, A. J. Austin, R. Cammi, C. Pomelli, J. W. Ochterski, R. L. Martin, K. Morokuma, V. G. Zakrzewski, G. A. Voth, P. Salvador, J. J. Dannenberg, S. Dapprich, A. D. Daniels, Farkas, J. B. Foresman, J. V. Ortiz, J. Cioslowski, and D. J. Fox, Gaussian, Inc., Wallingford, CT, 2009.